

---

EFDA–JET–PR(05)01

G.Gorini, H.Sjöstrand, S.Conroy, G.Ericsson, L.Giacomelli, H.Henriksson,  
A.Hjalmarsson, J.Källne, D.Palma, S.Popovichev, M.Tardocchi, M.Weiszflog  
and JET EFDA contributors

# Triton Burn Up Neutron Emission in JET Low Current Plasmas



# Triton Burn Up Neutron Emission in JET Low Current Plasmas

G. Gorini<sup>1</sup>, H. Sjöstrand<sup>2</sup>, S. Conroy<sup>2</sup>, G. Ericsson<sup>2</sup>, L. Giacomelli<sup>2</sup>, H. Henriksson<sup>2</sup>,  
A. Hjalmarsson<sup>2</sup>, J. Källne<sup>2</sup>, D. Palma<sup>1</sup>, S. Popovichev<sup>3</sup>, M. Tardocchi<sup>1</sup>, M.  
Weiszflog<sup>2</sup> and JET EFDA contributors\*

<sup>1</sup>*INFM, Dept. of Physics, Univ. of Milano-Bicocca, Milano, Italy and Istituto di Fisica del Plasma,  
EURATOM-ENEA-CNR Association, Milan, Italy*

<sup>2</sup>*INF, Uppsala University, EURATOM-VR Association, Uppsala, Sweden*

<sup>3</sup>*EURATOM/UKAEA Fusion Association, Culham Science Centre, Abingdon, Oxon, UK*

*\* See annex of J. Pamela et al, "Overview of JET Results ",  
(Proc.20<sup>th</sup> IAEA Fusion Energy Conference, Vilamoura, Portugal (2004)).*

"This document is intended for publication in the open literature. It is made available on the understanding that it may not be further circulated and extracts or references may not be published prior to publication of the original when applicable, or without the consent of the Publications Officer, EFDA, Culham Science Centre, Abingdon, Oxon, OX14 3DB, UK."

"Enquiries about Copyright and reproduction should be addressed to the Publications Officer, EFDA, Culham Science Centre, Abingdon, Oxon, OX14 3DB, UK."

## ABSTRACT

The dt neutron emission from JET H-mode deuterium discharges with  $Z_{\text{eff}} < 2.5$  and plasma currents  $1 < I_p < 3\text{MA}$  is analyzed on the basis of all neutron diagnostics information available on JET. This emission is mainly due to the triton burn-up process and is used to determine the fast triton confinement. A simplified model for Triton Burn-up Neutron (TBN) emission has been used and provides an adequate description of the dt emission. Prompt (first orbit) triton losses are found to amount typically to 50, 20 and 10% at  $I_p = 1, 2$  and  $3\text{MA}$ , respectively. Additional losses (such as losses due to “neoclassical” Coulomb collisions) may also play a role especially at the lowest current values.

Neutron emission spectroscopy measurements with the MPR spectrometer have detected a contribution to the dt emission due to residual tritium. Tritium concentration tends to increase with increasing impurity content being at the 15% level for the selected (low  $Z_{\text{eff}}$ ) discharges analyzed in this paper. For the higher  $Z_{\text{eff}}$  values frequently observed in JET the TBN analysis faces a number of difficulties and more direct approaches for fast ion studies should be considered.

## INTRODUCTION

The study of fast charged fusion reaction products in high temperature plasmas is of intrinsic interest and has an important bearing on the physics of fusion  $\alpha$ -particles. In particular, 1-MeV tritons from the  $d + d \rightarrow t + p$  reaction have similar orbits to 3.5MeV  $\alpha$ 's, which makes them suitable for simulation of certain  $\alpha$  particle confinement properties, e.g. prompt losses. For this reason TBN have long been used to infer the confinement properties of  $\alpha$  particles in the JET tokamak [1-2]. Only confined tritons can contribute to the TBN emission. Hence triton losses will lead to a reduction in the TBN emission, which can be observed experimentally.

For a given plasma device, triton losses depend mainly on the plasma current. The TBN studies carried out on JET in the '80s [1] explored mainly the plasma current range 3-6MA, representing very high confinement conditions compared to those of previous studies on smaller devices [3-6]. In more recent years, new plasma regimes have been investigated on JET with plasma currents in the range 1-3MA. This provides a new plasma operation range where fast ion confinement can be investigated experimentally, e.g. by TBN studies. A further motivation for TBN studies on JET is the general improvement of the neutron emission and other plasma diagnostic measurements leading to more accurate TBN analysis than previous studies could attain.

In this paper the results of analysis of TBN measurements in low current H-mode plasmas of JET are presented. The data refer to the period October 2000-May 2002. These plasmas provide a benchmark for TBN studies at low plasma currents in so far as they indicate the accuracy that these studies can achieve in terms of comparison between experiment and theory, and the required plasma conditions. A unique feature of JET is the presence of residual tritium from previous dt experiments, which contributes to the total dt neutron emission. This was regularly monitored using neutron spectrometry to ensure a correct interpretation of the TBN results.

## 1. THE TRITON BURN-UP MODEL

The triton burn-up process has been extensively described in the past so it will only be briefly reviewed here. It is important to point out some approximations underlying the so-called ‘‘classical’’ TBN model.

### 1.1 OVERVIEW OF THE TBN PROCESS

The TBN emission is the combined result of triton production, confinement, slowing down and burn-up. Triton burn-up is manifested in the 14MeV TBN emission intensity and its time evolution. Comparison of measured and theoretical time-resolved TBN emission is performed here with the help of a model describing the TBN process.

Tritons of 1.01MeV average energy are created in the reaction  $d+d \rightarrow t+p$  at the same rate as the routinely measured 2.5MeV neutrons from the  $d+d \rightarrow {}^3\text{He}+n$  reaction. The fraction of these tritons that are lost promptly depends on the plasma geometry and on the plasma current, and can be calculated by simulating the particle orbit motion in the plasma.

The tritons describe orbiting trajectories with a Larmor radius (LR) determined by

$$L_R = 0.33 p/(qB)$$

where LR is in centimetres, the momentum  $p$  in MeV/c, the magnetic field in tesla and  $q$  is the charge number. This gives 7.2cm for a field of 3.4T. As usual orbits can be circulating or trapped and their width increases in inverse proportion to the poloidal magnetic field; therefore the orbits are better confined in a high-current plasma. Some tritons hit the plasma first wall during their first orbit and are lost. This kind of losses is referred to as ‘‘prompt’’ since it takes place on the time scale of the orbit period, which is of the order of microseconds.

A useful quantity describing the confining properties of plasmas is the triton confined fraction  $f_c$ . This is the fraction of tritons that is not lost due to prompt losses. For fixed plasma geometry,  $f_c$  increases with current and decreases with increasing width of the triton emissivity profile. On JET,  $f_c$  is close to unity for plasma currents above 3MA.

The fast tritons confined in the plasma are slowed down to thermal energies through Coulomb collisions. The slowing down equation for fast ions is [7]

$$-\dot{W} = \frac{\alpha}{\sqrt{W}} + \beta W$$

where  $W$  is the triton energy and the coefficients are determined from the general expressions for the slowing down due to ions and electrons. These are

$$-\dot{W}|_i \cong - \left[ \frac{\frac{3}{2} \pi q_e^4}{m_p^{\frac{1}{2}}} \right] -\ln \Lambda_i Z^2 A^{\frac{1}{2}} \sum_j \frac{n_j Z_j^2}{q_j} \frac{1}{\sqrt{W}} \equiv - \frac{\alpha}{\sqrt{W}}$$

$$-\dot{W}|_e \cong - \left[ \frac{16}{3} \sqrt{\frac{\pi}{2}} \frac{q_e^4 m_e^{\frac{1}{2}}}{m_p} \right] -\ln \Lambda_e \frac{Z^2}{A} \frac{n_e}{T_e^{\frac{3}{2}}} W \equiv - \beta W$$

where  $Z, A$  are the triton charge and mass number,  $n_j, Z_j, A_j$  are the density, charge and mass number of each ion species in the plasma,  $q_e$  is the electron charge,  $m_e$  is the electron mass,  $m_p$  is the proton mass and  $\ln\Lambda_e$  and  $\ln\Lambda_i$  are the electron and ion Coulomb logarithm, respectively. Expressing energy and temperature in eV and all other quantities in cgs units, the numerical values of the coefficients in square brackets are  $1.81 \times 10^{-7}$  for the ions and  $3.18 \times 10^{-9}$  for the electrons.

For the special case of constant coefficients the slowing down equation can be integrated to determine the time  $t$  at which the triton energy is reduced from its initial energy  $W_0$  to a chosen energy  $W_f$ :

$$t(W_f) = \frac{2}{3} \frac{1}{\beta} - \ln \frac{\frac{\alpha}{\beta} + W_0^{\frac{3}{2}}}{\frac{\alpha}{\beta} + W_f^{\frac{3}{2}}}$$

The triton slowing down time is defined as the time  $\tau_s$  at which  $\tau_s \equiv t(W_f \equiv ET_i)$ . This introduces a logarithmic dependence on the ion temperature  $T_i$ . In practice, since  $T_i$  is often close to  $T_e$ , the  $T_i$  dependence mitigates the  $T_e^{3/2}$  dependence from  $\beta$  and a practical scaling of the slowing down time is  $\tau_{SD} \sim T_e/n_e$ . The slowing down time is not used for the TBN analysis but its value and scaling are useful for estimates. 1MeV tritons are slowed down on the time scale 0.1-1s for typical JET plasma conditions.

During the slowing down, a fraction of the confined tritons undergo nuclear fusion (burn-up) reactions  $t+d \rightarrow \alpha+n$ , which is manifested in the 14MeV TBN emission. The effective dt cross section is peaked at a triton energy of 170-200keV depending on the deuteron temperature [8]. As a result, the burn-up probability peaks with a time delay (relative to the birth time) of the order of the slowing down time. This is reflected in a characteristic delay of the TBN emission relative to the dd neutron emission. This delay is an important observable to be reproduced in the simulations.

The 14 to 2.5MeV neutron production ratio, which is the triton burn-up fraction  $\rho$ , is a function of the slowing down of the tritons as well as of their containment. The comparison between the measured burn-up fraction,  $\rho_{exp}$ , and the theoretical burn-up fraction,  $\rho_{th}$ , provides an inclusive means to test the classical TBN model. This was the main objective of early TBN studies [1]. Since the 14MeV neutron emission can be measured with adequate time resolution on JET [2], a more detailed comparison of measured and simulated time-resolved TBN emission is also possible and is performed here to provide a more accurate test of the classical TBN model. Finally, the TBN has a characteristic neutron emission spectrum [9]; this is essential in order to identify the TBN emission unambiguously and distinguish it from other 14-MeV neutron emission processes due to residual tritium contamination of JET (see below).

The level of detail for modeling the TBN process depends on the desired accuracy level. Since the TBN data have uncertainties at the 10% level and, furthermore, the TBN model depends on plasma parameters with uncertainties at the 10-20% accuracy level, we set at the 10% level the accuracy of the TBN model. In this way many details of the TBN process can be simplified or completely disregarded.

It is interesting to observe that a coarse scaling of the burn-up fraction is  $\rho \sim f_c \times T_e \times n_e/n_d$ . Thus the uncertainties in  $T_e$  and in the density ratio  $n_d/n_e$  will propagate linearly to the result of any TBN model simulation, no matter how accurate the model is. On the other hand, the characteristic time delay of the TBN emission scales as  $T_e/n_e$ . The combined availability of observables with different parametric dependencies is sometimes useful here for validating the accuracy of the input plasma parameters used in the simulations.

## 1.2 MODEL ASSUMPTIONS

The starting point of the triton burn-up model calculation is the time-resolved “birth” distribution of tritons in the available phase space. It is assumed that the triton velocity distribution is isotropic; this is not true for plasmas with NBI and/or ICRH heating but the resulting error in the TBN emission is small [10]. Another approximation is to replace the individual triton energy with the average energy of 1.01MeV. The triton energy spectrum is broadened due to the kinetic energy of the reacting deuterons, but this has little consequence for the TBN process. There is also a small spectral shift [11], which is disregarded here. As for the triton emissivity profile, this is assumed to be a magnetic flux function; i.e. it is uniform over the magnetic flux surfaces.

Since the two branches of the dd fusion reaction have equal probability, the 2.45MeV neutrons and the 1.01MeV tritons have the same birth profile. Therefore the dd neutrons provide a means to determine the triton birth profile experimentally using the time resolved data from the neutron camera system (see below).

Individual tritons orbits are calculated without any approximation to determine the triton confined fraction  $f_c$ . In principle  $f_c$  varies with time for transient plasma conditions but, for the purpose of this work,  $f_c$  is determined once per plasma discharge.

The slowing down of tritons is calculated taking into account the time dependence of  $T_e$  and  $n_e$  as provided by diagnostic measurements. There is also a spatial dependence of the  $T_e$  and  $n_e$  values, which vary along each triton orbit. The approximation made here is to model the effect of the orbital excursion by broadening the triton birth profile (i.e. by redistributing the tritons over a radial width chosen here to be 10% of the plasma minor radius) after which the tritons are assumed to slow down where they are born.

An effect that is not included in the present TBN model is the occurrence of triton losses during the slowing down process. These are referred to as delayed losses. An example is the so-called neoclassical losses due to triton deflections by Coulomb collisions resulting in a change of orbit. These losses have been recently investigated numerically especially in relation to alpha particle confinement in plasma equilibria with a current hole [12].

The actual triton burn-up (where the triton undergoes a fusion reaction and emits a 14MeV neutron) occurs with a probability given by the expression

$$dp/dt = \sigma_{dt} n_d v$$

where  $\sigma_{dt}$  is the dt cross section,  $n_d$  is the deuterium density and  $v$  is the triton velocity.

The time dependence of  $\sigma_{dt} n_d$  and  $v$  as the triton slows down is taken into account without any approximation but  $\sigma_{dt}$  is calculated assuming the deuterons are at rest. The spatial dependence of  $nd$  is dealt with in the same way as is done for  $T_e$  and  $n_e$  in the slowing down.

Since the density ratio  $n_d/n_e$  is not a directly measured quantity it must be derived from other experimental data. Here we determine  $nd/n_e$  from  $Z_{eff}$  as provided by visible bremsstrahlung. It is further assumed that  $Z_{eff}$  and  $n_d/n_e$  are uniform and that one impurity species (usually carbon) of charge number  $Z$  is dominant. Under these assumptions the density ratio is related to  $Z_{eff}$  by

$$n_d/n_e = (Z_{eff}-Z)/(1-Z)$$

This is further corrected for the presence of small admixtures of hydrogen and beryllium at the % level.

### ***1.3 NUMERICAL CODES***

The simplified TBN model used for the data analysis is implemented by two separate simulation codes. The triton confined fraction,  $f_c$ , is determined once per plasma discharge from first-orbit simulations performed with the Monte Carlo code McOrbit. The code uses the experimental magnetic equilibrium and neutron emissivity profile to calculate the triton orbits. Examples of McOrbit calculations are shown in Fig.1 and 2. These are so-called “fat banana” orbits of tritons in plasmas with different currents. For comparison  $\alpha$ -particle orbits are also shown. Note that McOrbit calculates the exact trajectory and not its guiding centre approximation. One can see that these orbits are very wide and indeed are not confined in the low current case. By generating a large number of these orbits the triton confined fraction,  $f_c$ , is determined. Typically 30,000 orbits are launched. The code can be used for more detailed studies, an example being shown in Fig.3, which features the computed radial distribution of the tritons that are lost to the wall.

The second code used for TBN simulation is called TRAP-T. It was developed in the late 80’s [2] and is still in use. It calculates the time evolution of the TBN emission assuming no triton losses using the assumptions described earlier. Each triton is assumed to slow down and react at its birth point; i.e. no orbit effect is included in the simulation, but the  $dd$  emissivity and other plasma parameter profiles affecting the triton slowing down are taken into account. For this purpose the model divides the plasma in a number of toroidal shells with  $T_e$ ,  $n_e$  and neutron emissivity specified by diagnostic measurements (usually the LIDAR Thomson scattering system and the neutron cameras). The concentration factor is derived from  $Z_{eff}$ . The model is time dependent and allows one to determine the TBN yield as a function of time. The model was used extensively for the high current (above 3MA) plasmas of JET [2] where triton losses could hardly be observed. Here we extend its use for currents as low as 1MA by combining it with independent calculations of the triton confined fraction, which, however, must not vary in time and space. The systematic error introduced by neglecting the spatial variation of the losses (see Fig.3) is further addressed in §6.

## 2. EXPERIMENT

The measurements analyzed in this paper were carried out in the period October 2000-May 2002. During this period JET was operated in different modes and here we analyze discharges most of which were intended to achieve H-mode conditions. These discharges have long periods of nearly steady-state conditions. Time traces of a typical discharge are shown in Fig.4. All data have uncertainties at the 10-20% level except for the NBI power. Some of the data shown are a subset of the data used as an input for the TRAP-T simulations. This includes the total (dd+dt) neutron yield measured by a set of fission chambers, which practically coincides with the dd yield since the dt contribution is at the 1% level. Neutron emissivity profiles (not shown) were also measured routinely with the two JET neutron cameras and used in the simulations. The dt neutron yield was measured with a silicon detector that works on the following principle. The (n,  $\alpha$ ) and (n, p) reactions in silicon can be used for monitoring the 14MeV dt neutron flux from JET discharges because the reaction thresholds ( $\sim 7$ MeV) are well above the 2.5MeV neutron energy from dd reactions. The energetic reaction products are retained within the silicon and produce signals much greater than those from simple scattering of neutrons and those due to gamma rays. Silicon diodes are therefore suitable for monitoring the 14MeV neutron emission at all intensities, from triton burn-up to full dt plasma experiments, with limitations due to radiation damage. At JET for dd-plasma a Si detector with 450mm<sup>2</sup> active area and 1 mm sensitivity depth is usually in use for TBN measurements. It is located near a main horizontal port, at about 3.5m from the centre of plasma.

All neutron measurement systems are calibrated by comparison with absolute, time-integrated neutron measurements performed with an activation system. An example of calibrated dd and dt time traces is shown in Fig.5, which also shows the result of a TRAP-T simulation. The agreement between data and simulation is impressive in this particular example.

The yield and emissivity measurements are complemented by neutron spectrometry measurements of 14 MeV neutrons performed with the MPR spectrometer [13]. These measurements have the important task of establishing the presence of dt neutron emission processes different from TBN. The MPR rates are very low in deuterium plasmas and data from many (of order 100) plasma discharges need to be added to achieve adequate statistics. Under these conditions the MPR is set so that the spectrum of the Analogue to Digital Converter (ADC) for each hodoscope detector is recorded. An example of ADC spectrum is shown in Fig.6(a). It features a high-energy peak above channel 400 due to protons depositing their full energy in the scintillator. The intensity of this peak and similar peaks in ADC spectra of other hodoscope detectors is plotted in the form of a position histogram in Fig.6(b). This histogram is finally analyzed by folding the detector response with model neutron energy spectra. This method has been used previously for low rate observations and is known to provide data with accuracy at the 5% level. However for some of the channels the data were of too poor quality and they could not be included in the analysis.

### 3. MEASUREMENTS AND ANALYSIS

#### 3.1 DATA SELECTION

A set of 112 discharges was selected from a total of hundreds by applying a few selection constraints. First, a practical threshold of  $2 \times 10^{15}$  in the total neutron yield was imposed in order to achieve sufficient statistics in the 14MeV neutron measurements. Second, only plasmas with  $Z_{\text{eff}} < 2.5$  were included in the analysis. The reason for this threshold in  $Z_{\text{eff}}$  is the uncertainty in the  $n_d/n_e$  ratio. Higher  $Z_{\text{eff}}$  values mean larger uncertainties in  $n_d/n_e$ , which propagate linearly to the simulated burn-up fraction. Finally, some discharges had to be rejected because of the poor quality of some diagnostic data required for the analysis.

The data set selected for analysis covers the range of plasma currents 1-3MA. The data show some variability in this range as illustrated by the measured burn-up fraction values,  $\rho_{\text{exp}} = N_{\text{dt}}/N_{\text{dd}}$ , where  $N_{\text{dt}}$  and  $N_{\text{dd}}$  are the total (time integrated) 14 and 2.5MeV yields. The  $\rho_{\text{exp}}$  values are plotted in Fig.7 as a function of plasma current. The data show a trend given approximately by  $\rho_{\text{exp}}[\%] = I_p[\text{MA}]/2$  and a large scatter around this trend. The current dependence of  $\rho_{\text{exp}}$  is mainly a manifestation of a well-known correlation between plasma current and electron temperature.

#### 3.2 RESULTS OF DATA ANALYSIS

Code simulations were run for all plasma discharges in the data base. An example where the agreement between simulation and data is remarkable was shown in Fig.5. This was a 2.6MA discharge for which we expect most of the triton to be confined. Another example of a high current discharge is shown in Fig.8. One can see that the agreement is very good regardless of the detailed shape of the dd neutron time trace. Especially the Ttransients in the TBN trace are well reproduced, indicating that the relevant input data and the model assumption have adequate accuracy.

At lower plasma currents the TRAP-T simulation is systematically above the experiment. This is not surprising and we expect it to be explained in terms of triton losses not included in the TRAP-T simulation. An example is shown in Fig.9 where the plasma current is rather low. To be noted is also the lower statistics of the experimental dt trace which is typical of low current plasmas and can be appreciated by the larger scatter in the data. The log scale plot shows that a scale factor can account for the mismatch between simulation and data; however the statistics is too low to provide conclusive evidence in the rise and fall phases of the dt neutron emission, which would be most sensitive to deviations from the model assumptions.

Evidence of triton losses manifests itself in the TBN data by taking the ratio  $\rho_{\text{exp}}/\rho_{\text{sim}}$  between the experimental  $\rho_{\text{exp}}$  values and corresponding simulated value  $\rho_{\text{sim}}$  from TRAPT, which assumes no losses. The ratio is plotted in Fig.10 vs plasma current for the same plasma discharges of Fig.7. The dashed line marks the unity ratio expected under conditions of perfect triton confinement. Open and full triangles are for total dd neutron yields below and above  $10^{16}$  neutrons, respectively. No obvious correlation of the ratio with the neutron yield is observed, but a clear current dependence is seen. A similar current dependence is found (Fig.11) in the confined fraction,  $f_c$ , determined from

orbit simulations using the McOrbit code. Losses at the 50% level are found to be typical of 1MA plasmas; at 2 and 3MA the losses are about 20% and 10%, respectively. There is some scatter of the  $f_c$  values about the average current dependence, which can be attributed to various causes including different neutron emissivity profiles for the same total plasma current. Before drawing conclusions from the data of Fig.10 and 11 we must however consider the contamination of the dt neutron data by residual tritium.

#### 4. THE ROLE OF RESIDUAL TRITIUM

Neutron spectrometry provides evidence of a non-negligible amount of dt neutrons emitted by residual tritium. Fig.12 shows the analysis of a intensity hystogram (here the scale is converted to proton energy) in terms of components of the neutron spectrum obtained by adding data from a large number (over 300) discharges for the period of interest for which data are available. The fitted line is the sum of a broad component of known shape [9] from Triton Burn Up (TBN) and a narrow component (labeled Thermal) that is assumed to be of thermonuclear shape (i.e., Gaussian [11]). There is also a third component due to neutron scattering affecting the low energy side of the spectrum. The Thermal component is attributed to residual tritium from previous dt experimental campaigns [13]. This residual tritium component has been observed to decrease with time over the 6-year period following the dt experiments in 1997. The TBN/(Thermal+TBN) ratio for this data set is  $\eta=0.68$ . In other words, about one third of the dt neutron emission was not due to triton burn-up in the time period of these measurements. Clearly this is an important contribution to the total dt rate and must be investigated in more detail. This is done in Fig.13, which shows the neutron spectrum obtained by adding up data from discharges belonging to the data set of the TBN analysis. The statistics is worse but sufficient to prove that the residual tritium emission is about 15%. This is about a factor of two lower than the average value for that period, which could be explained if we assume that plasmas with higher  $Z_{\text{eff}}$  have also a higher content of residual tritium. The TBN data set has  $Z_{\text{eff}} < 2.5$  and a 15% neutron yield from residual tritium, whereas higher average values of both  $Z_{\text{eff}}$  and residual tritium are found in the enlarged data set. No other evidence of a correlation of the residual tritium content with plasma operation and conditions has previously been reported.

The 15% average contamination level of the dt yield from residual tritium must be included in the TBN analysis of the previous section. Actually one wonders how a 15% contribution can go undetected in the time trace analysis. Indeed the TBN (from burn-up) and Thermal (from residual tritium) dt yields have different time traces. The TBN is delayed relative to the dd emission whereas the Thermal dt emission should more or less follow the dd neutron time trace. This should provide a way, independent from neutron spectrometry, to separate the two neutron emission components. It turns out that the sensitivity level of the time trace analysis is not good enough. Fig.14 shows an expanded view of the measured and simulated dt yield for JET plasma Pulse No: 52958 (from Fig.5). Also shown is the simulated dt time trace for a model case where 30% of the total dt neutron emission is assumed to be Thermal. As one can see, a 30% admixture would be detectable, whereas

a 15% admixture gives a time trace (not shown) that is practically undistinguishable from the pure TBN case.

The effect of an average 15% residual tritium contribution to the dt yield is to raise the “perfect agreement” line in Fig.7 to the level marked by a full line. With this effect taken into account the data show that the experimental TBN yield is roughly half of what expected at  $I_p = 1\text{MA}$  and approaches the expected value at the highest currents. This is in fair agreement with the  $f_c$  trend of Fig.11.

A more quantitative comparison of the current dependences seen in Figures 10 and 11 is obtained by introducing a corrected burn-up fraction  $\rho_{\text{exp}}' = (N_{\text{dt}}/N_{\text{dd}}) * \eta$  and the corresponding simulated quantity  $\rho_{\text{sim}}' = \rho_{\text{sim}} * f_c$ . The ratio  $\rho_{\text{exp}}'/\rho_{\text{sim}}'$  is shown in Figure 14.

The ratio is convincingly close to unity at high current. At lower currents the data are scattered but suggest  $\rho_{\text{exp}}' < \rho_{\text{sim}}'$  by 10-20% (although  $\rho_{\text{exp}}'/\rho_{\text{sim}}' = 1$  is not incompatible with the data given the large uncertainties). Neoclassical triton losses [12] are a likely mechanism for additional reduction of TBN at low currents. Is it also possible that some additional losses of tritons at low current could be due to MHD activity such as described in [14]. One should also bear in mind the limitations introduced by the model assumptions. Especially the assumption of uniform triton losses across the plasma seems questionable with a 50% loss level. This, however, cannot explain a  $\rho_{\text{exp}}' < \rho_{\text{sim}}'$  result because the burn-up probability is larger in the (hotter) plasma core. Hence the model tends to underestimate the TBN emission, which leads us to believe that there may indeed be additional triton losses at a level that is best investigated by a more sophisticated model than the one used in the present analysis.

## CONCLUSIONS

The dt neutron emission from H-mode deuterium discharges with  $Z_{\text{eff}} < 2.5$  and plasma currents  $1 < I_p < 3\text{MA}$  has been studied on the basis of all neutron diagnostics available on JET. A simplified model for Triton Burn-up Neutron (TBN) emission has been used and provides an adequate description of the dt emission. Prompt (first orbit) triton losses are found to amount typically to 50, 20 and 10% at  $I_p = 1, 2$  and  $3\text{MA}$ , respectively. Below  $2\text{MA}$  additional losses (such as due to “neoclassical” Coulomb collisions) could also play a role and should be investigated theoretically.

Neutron emission spectroscopy measurements with the MPR spectrometer have detected a contribution to the dt emission due to residual tritium. Its concentration tends to increase with increasing impurity content being at the 15% level for the selected (low  $Z_{\text{eff}}$ ) discharges analyzed in this paper. This level does not preclude a useful TBN analysis. For the higher  $Z_{\text{eff}}$  values frequently observed in JET the TBN analysis faces a number of difficulties and more direct approaches for fast ion studies should be considered, that are not dependent on detailed knowledge of the tritium contamination of the plasma and the deuterium density ratio.

## ACKNOWLEDGEMENT

This work was carried out within the framework of the European Fusion Development Agreement. The views and opinions expressed herein do not necessarily reflect those of the European Commission.

## REFERENCES

- [1]. J.Källne, P.Batistoni, G.Gorini, G.B.Huxtable, M.Pillon, S.Podda, M.Rapisarda,( Triton Burn-up Measurements at JET Using Neutron Activation Technique), Nucl.Fusion **28** (1988)7, 1291.
- [2]. S. Conroy, et al., Nucl. Fusion **28** (1988) 2127; S. Conroy, Ph. D. Thesis, Imperial College (1990).
- [3]. Heidbrink,W.W., Chrien,R.E., Strachan,J.D., Nucl. Fusion **23** (1983) 917.
- [4]. Strachan,J.D., Chan,A.A., Heidbrink,W.W., et al, in Basic Physical Processes of Toroidal Fusion Plasmas (Proc. Workshop Varenna, 1985), Vol.2, CEC, Brussels (1986) 699.
- [5]. Batistoni,P., Martone,M., Pillon,M., Podda,S., Rapisarda,M., Nucl. Fusion **27** (1987) 1040.
- [6]. Pillon,M., Vannucci,P., Nucl. Instr. and Meth. A 255 (1987)188.
- [7]. Stix,T.H., Plasma Phys. **14** (1972) 367.
- [8]. G.Gorini, L.Ballabio, J.Källne, (Neutron Spectrometry Diagnostic of Triton Burn-up in Deuterium Fusion Plasmas), Plasma Phys. and Contr. Fusion **39** (1997) 61.
- [9]. L.Ballabio et al, Nucl. Fusion **40** (2000) 21.
- [10]. G.Gorini, P.Batistoni, E.Bittoni, J.Källne, S.Podda and A.Taroni, (Calculation of the Classical Triton Burn-up in JET Deuterium Plasmas), JET Report JET-P(87)35, JET Joint Undertaking, Abingdon, Oxfordshire (1987).
- [11]. L.Ballabio, J.Källne, G.Gorini, Nucl. Fusion **36** (1998) 1723.
- [12]. V.Yavorskij et al, Nucl. Fusion **43**, 1077 (2003)
- [13]. G.Ericsson, L.Ballabio, S.Conroy, J.Frenje, H.Henriksson, A.Hjalmarsson, J.Källne, M.Tardocchi (Neutron Emission Spectroscopy at JET – Results from the MPR Spectrometer), Review of Scientific Instruments **72** (2001) 759.
- [14]. F.B. Marcus, et al, (Effects of sawtooth crashes on beam ions and fusion product tritons in JET), Nucl. Fusion, 1994.

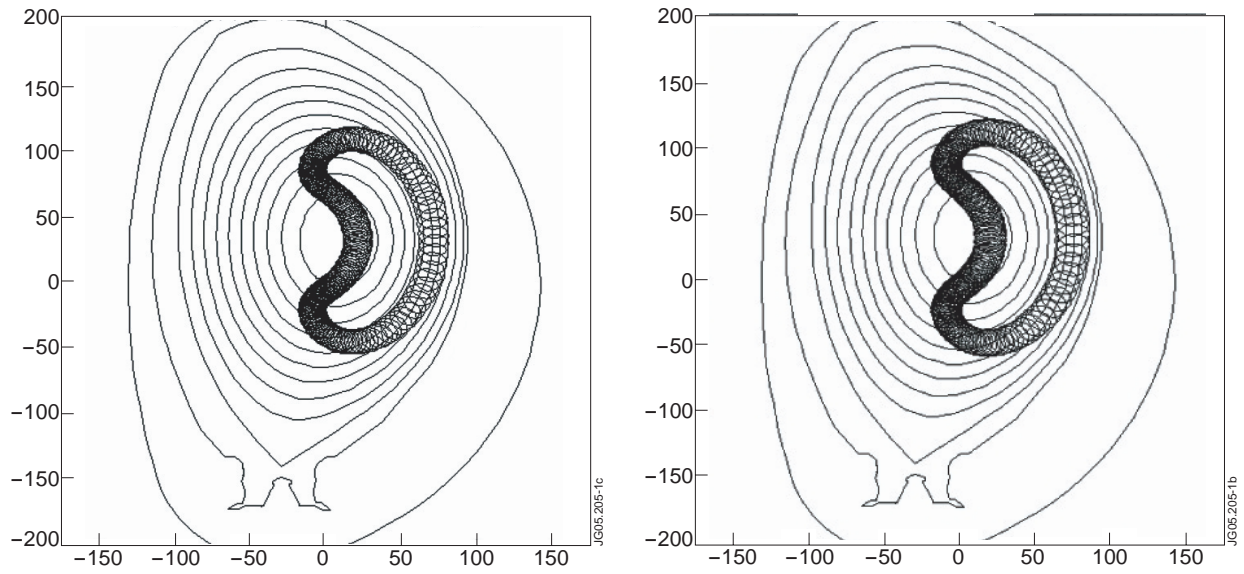


Figure 1: Example of “fat banana” orbits of a 1-MeV triton (a) and a 3.5 MeV  $\alpha$ -particle (b) with same initial position ( $x = 0\text{ cm}$ ,  $z = 3\text{ cm}$ ) and pitch angle ( $\theta = 75^\circ$ ). The magnetic equilibrium used in the simulation is taken from JET Pulse No: 52958 at time  $t = 21.86\text{ s}$ . The plasma current was 2.6 MA. The  $x$  and  $y$  coordinates are the distance in cm from the geometrical centre of the vacuum vessel.

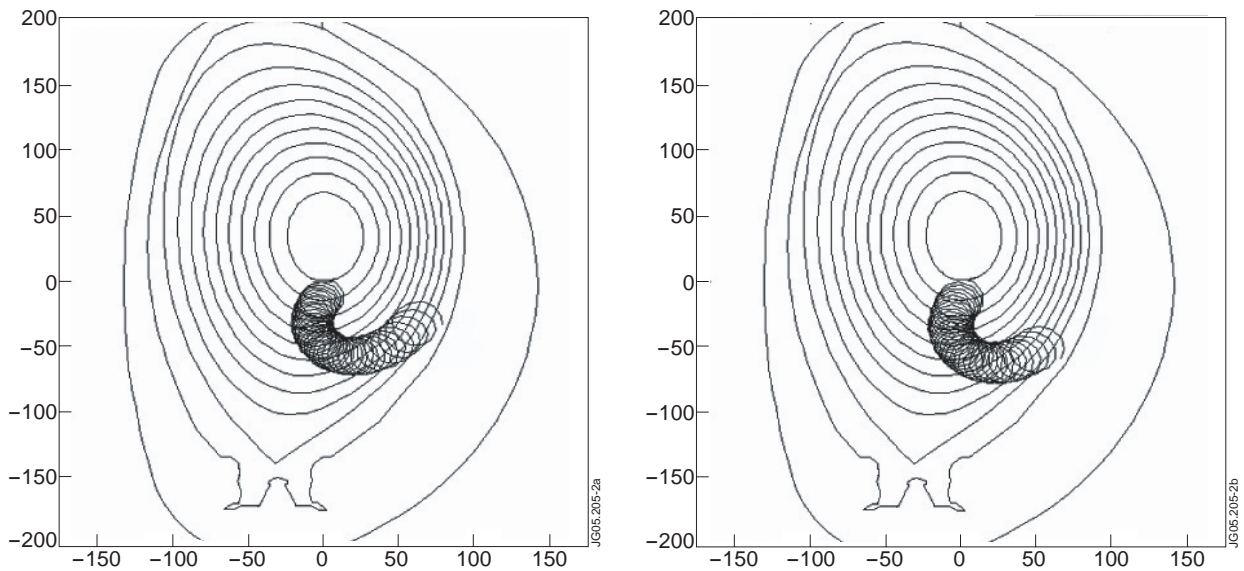


Figure 2: Same as Fig.2 but for a 1.6 MA discharge (Pulse No: 52771,  $t = 18\text{ s}$ ). The particles are no longer confined.

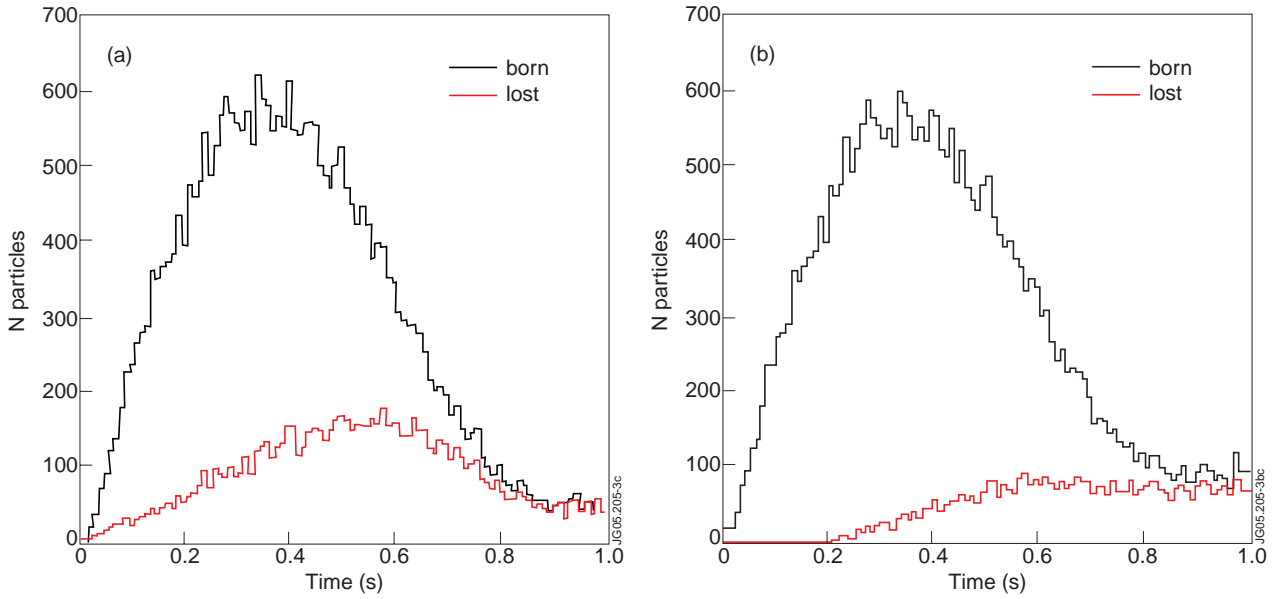


Figure 3: Examples of radial profiles of simulated tritons in JET plasmas at (a) low current (Pulse No: 52771 at  $t = 18$  s,  $I_p = 1.6$  MA, total losses 29%) and (b) high current (Pulse No: 52958 at  $t = 22$  s,  $I_p = 2.6$  MA, total losses 15%).

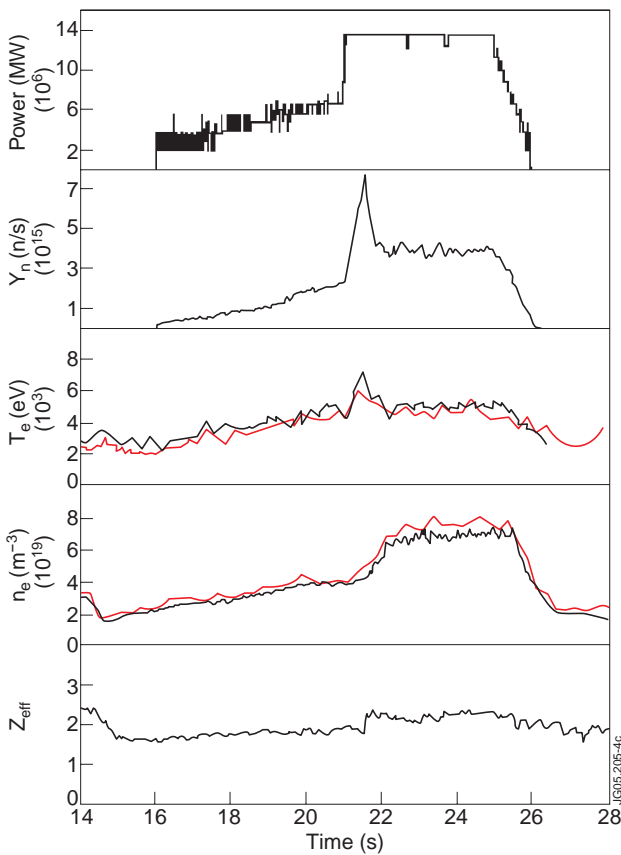


Figure 4: Time traces of some plasma parameters for JET Pulse No: 52958. This was an H-mode discharge with plasma current  $I_p = 2.6$  MA and toroidal magnetic field  $B_T = 2.6$  T. Shown are the traces of Neutral Beam Injection power, total neutron yield, peak electron temperature from LIDAR and ECE, peak density from LIDAR and interferometry, and  $Z_{eff}$  from visible bremsstrahlung.

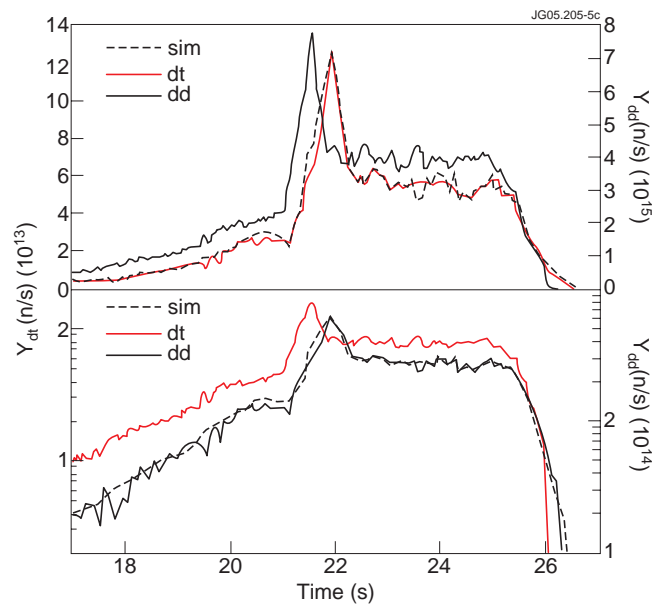


Figure 5: Time resolved  $dd$  (left) and  $dt$  (right) neutron yields for JET Pulse No: 52958 ( $I_p = 2.6$  MA) plotted on a linear (top) and log (bottom) scale. The dashed line is the simulated  $dt$  yield from triton burn up.

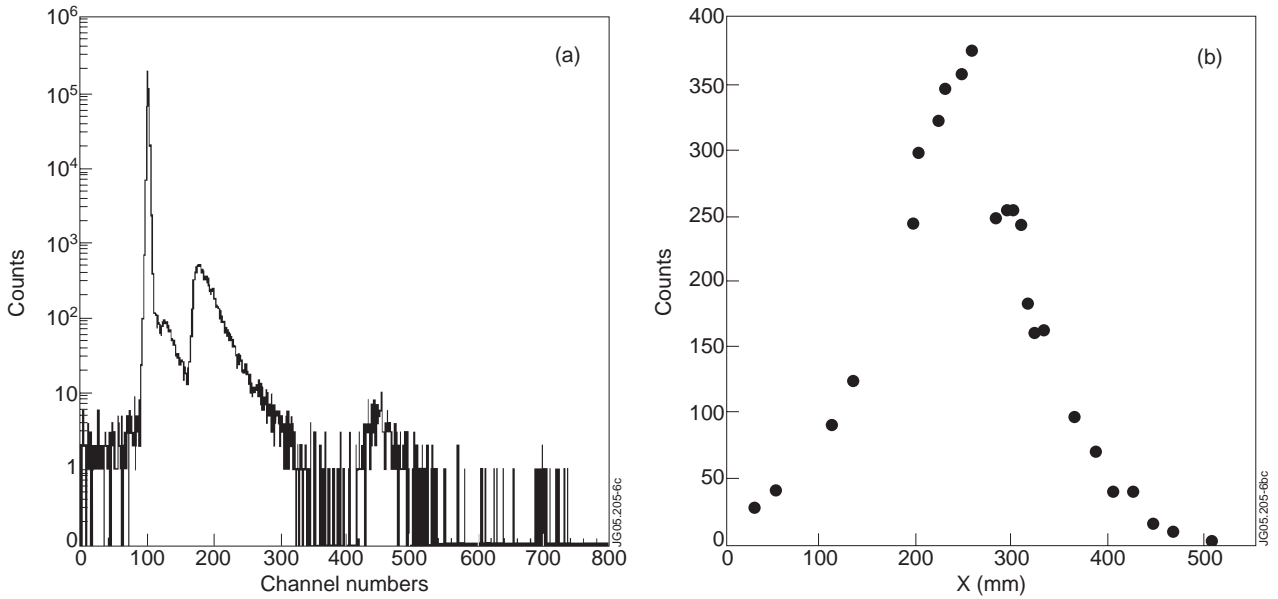


Figure 6: Examples of neutron spectrometry data. The data refer to all plasma discharges of TF-S1 for which MPR data were recorded. In (a) the ADC spectrum for hodoscope detector #17 (hodoscope coordinate  $X=248$  mm) features a well separated high energy peak above channel 400. The intensity of this peak and similar peaks in ADC spectra of other hodoscope detectors is plotted in (b) as a position hystogram.

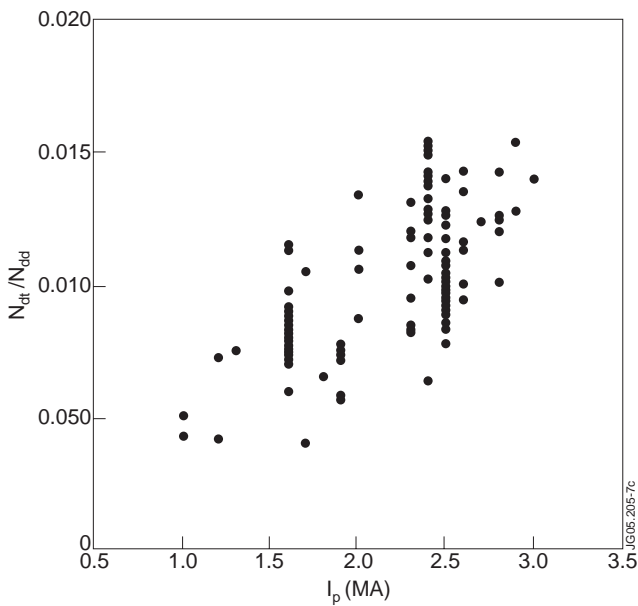


Figure 7: Ratio of dt and dd neutron yields from selected plasma discharges (see text) plotted versus plasma current.

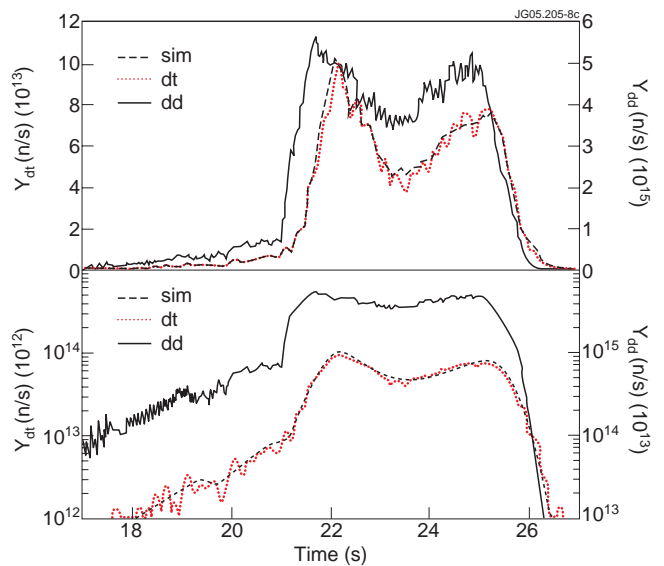


Figure 8: Time resolved dd (left) and dt (right) neutron yields for JET Pulse No: 53718 ( $I_p=2.5$  MA) plotted on a linear (top) and log (bottom) scale. The dashed line is the simulated dt yield from triton burn up.

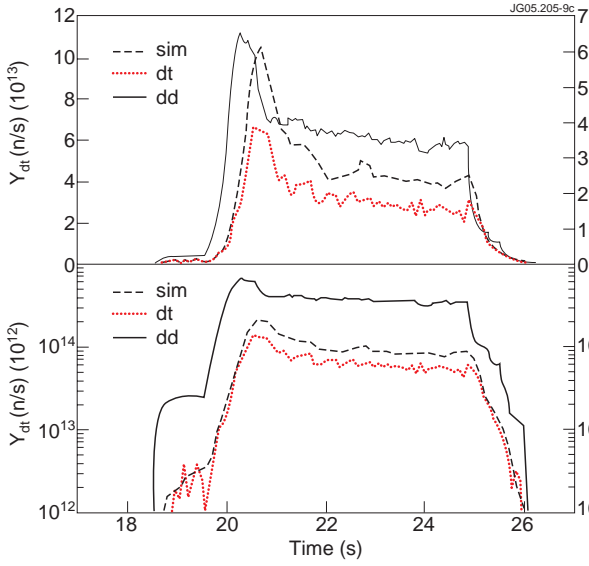


Figure 9: Same as Fig.8 but for JET Pulse No: 52771 ( $I_p = 1.6\text{MA}$ ).

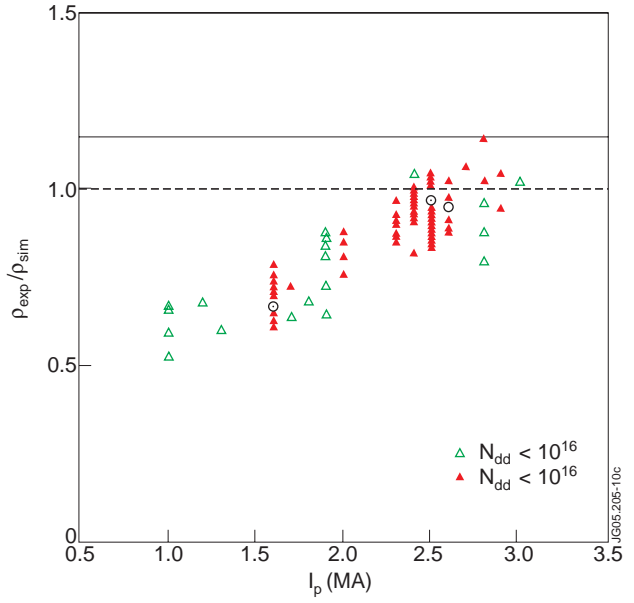


Figure 10: Ratio of experimental and simulated burn up fraction for the same plasma discharges of Fig.7 plotted vs plasma current. Open and full triangles are for total dd neutron yields below and above  $10^{16}$  neutrons, respectively. The circles mark the three discharges used as examples throughout the paper. The dashed line marks the unity ratio expected under conditions of perfect triton confinement. The full line marks the level expected due to contamination from residual tritium (see text).

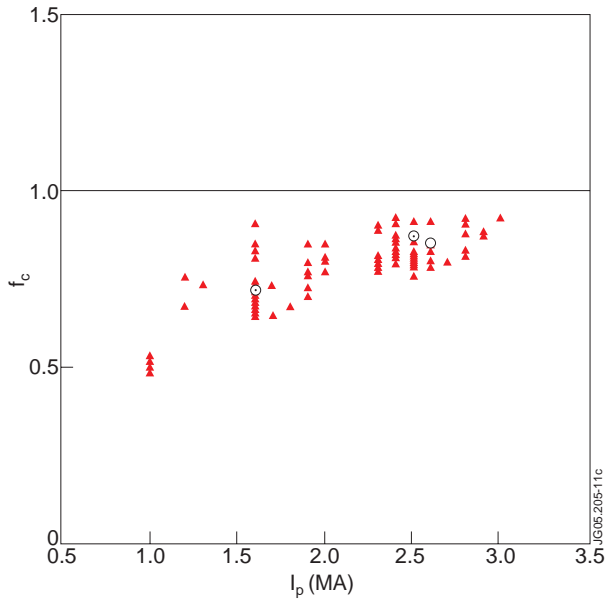


Figure 11: Confined fraction of tritons according to First Orbit simulations for the same plasma discharges of Fig.7 plotted vs plasma current. The symbols have the same meaning as in Fig.10.

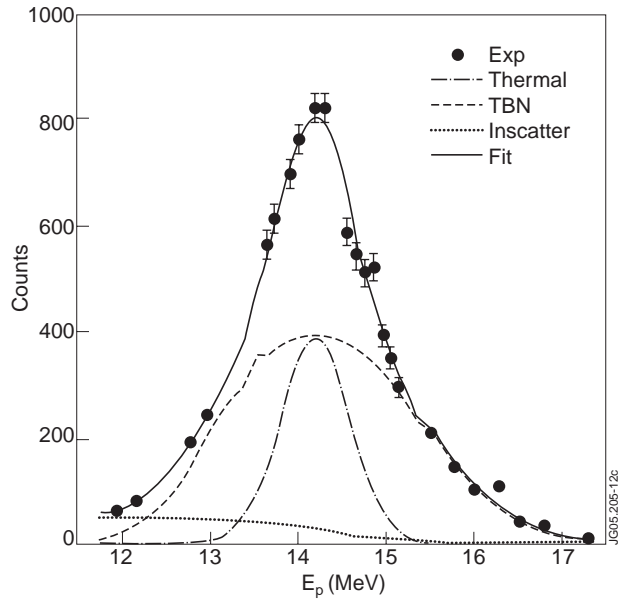


Figure 12: Analysis of neutron spectrum for an inclusive set of plasma discharges (see text). The fitted line is the sum of a broad component from Triton Burn Up (TBN) and a narrow component due to residual tritium (Thermal). There is also a third component on the right due to neutron scattering (Inscatter). The TBN (Thermal+TBN) ratio is  $\eta = 0.68$ .

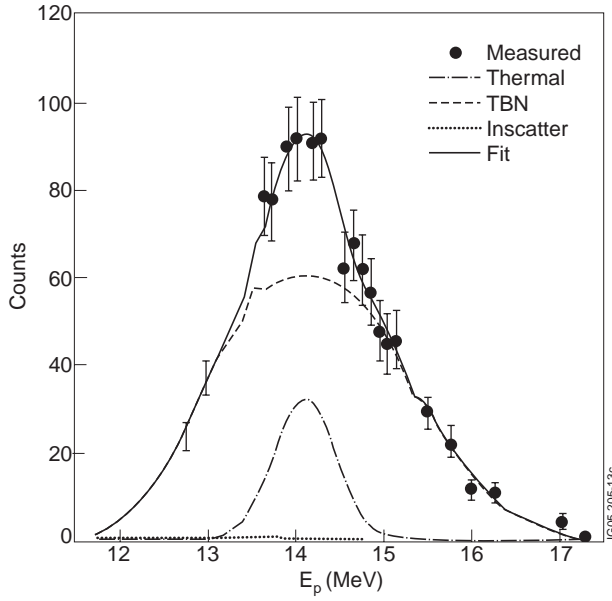


Figure 13: Same as Fig.12 but for a set of selected plasma discharges with  $Z_{eff} < 2.5$  (see text). The TBN/(Thermal + TBN) ratio is  $\eta = 0.82$ .

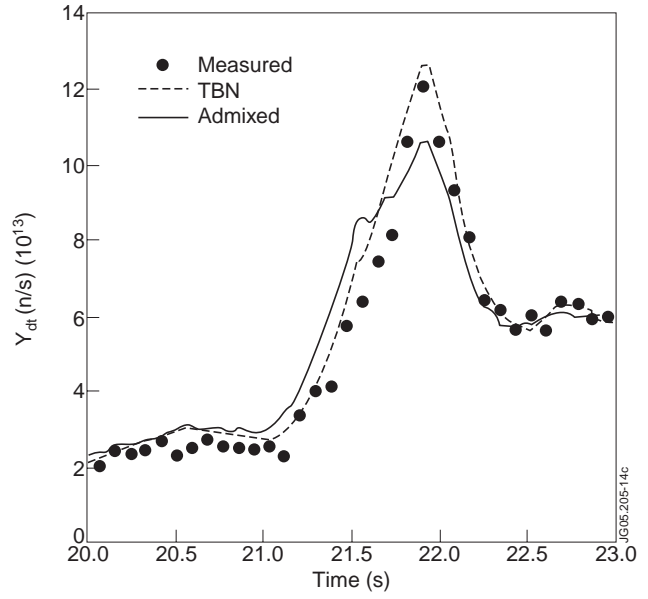


Figure 14: Expanded view of the measured and simulated dt yield for JET 52958 (from Fig.5). Also shown is the simulated dt time trace for a model case where 30% of the total dt neutron emission is due to residual tritium. The total dt yield is the same in both simulations.

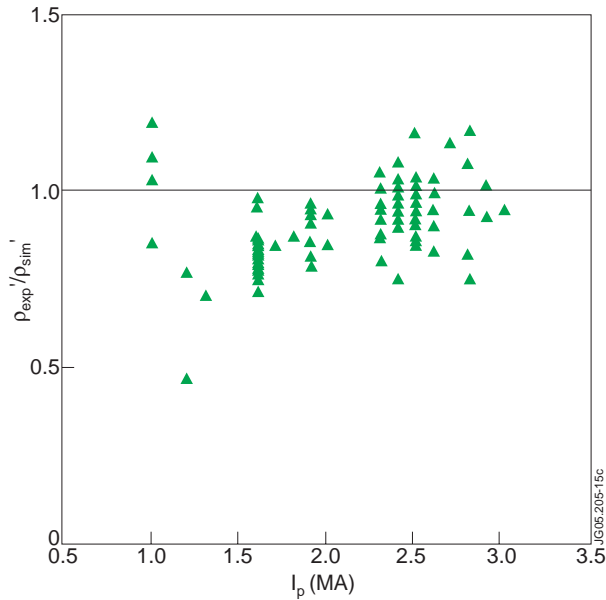


Figure 15: Ratio  $\rho_{exp}'/\rho_{sim}'$  for the same plasma discharges of Fig.7 plotted vs plasma current. Here  $\rho_{exp}' = \rho_{exp} * \eta$  and  $\rho_{sim}' = \rho_{sim} * f_c$  where  $\rho_{exp} = N_{dt}/N_{dd}$  and  $\rho_{sim}'$  are the (uncorrected) experimental and simulated burn up fractions, respectively,  $\eta = 0.85$  is a correction factor for residual tritium, and  $f_c$  is the confined fraction of tritons from Monte Carlo orbit simulation.